JOURNAL OF SOLID STATE CHEMISTRY **139,** 85–92 (1998)
ARTICLE NO. SC987814

Comparative Zirconium Bromide Cluster Chemistry. A New Structure in $K_4Zr_6Br_{18}C$

Ru-Yi Qi and John D. Corbett

Department of Chemistry, Iowa State University, Ames, Iowa 50011

Received September 22, 1997; in revised form March 4, 1998; accepted March 10, 1998

Reactions of $ZrBr_4$, Zr, ABr (A = Li–Cs, Ba), and Z (Be, B, C, Mn) mixtures with suitable compositions in sealed Ta containers have revealed 19 additional examples of $A_x(Zr_6Br_{12}Z)Br_y$-type phases that span $0 \le y \le 6$. A new triclinic structure is reported for $K_4Zr_6Br_{18}C$ ($P\bar{1}$, $Z = 1$, $a = 10.114(2)$, $b = 10.283(3)$, $c = 10.374(3)$, $\alpha = 118.54(2)$, $\beta = 99.98(2)$, $\gamma = 104.08(2)$, $R(F)/R_w = 5.1/4.7\%$) and $K_4Zr_6Br_{18}Fe$. Nearly octahedral $Zr_6(C)Br_{18}^{4-}$ clusters stack in layers with K^+ in pseudo-tetrahedral bromine cavities on their outward surfaces. The present structure can be converted to a pseudo-C-centered monoclinic version that is related to those of $Rb_4Zr_6Cl_{18}C$ ($C2/m$) and, more distantly, $Rb_5Zr_6Cl_{18}B$ ($Pnam$) according to cluster size and the need for good bonding sites for the cations. A variety of other new bromide phases that form in seven known zirconium cluster chloride or iodide structure types according to powder pattern or single crystal data is also reported. Some of these demonstrate greater, lesser, or alternative cation site occupancies in the same basic structure types. © 1998 Academic Press

INTRODUCTION

Transition metals of group 3 and 4 form a wide variety of $M_6X_{12}Z$-type clusters in which halide (X) has edge-bridging functions (1, 2). These always contain a heteroelement Z within each cluster that serves to augment the cluster electron count from these early metals. Z is apparently always bound in the center of the nominally octahedral metal clusters, except for a few cases with hydrogen. The great variety of compounds and structures containing these building blocks arises from several variables which relate to optimal bonding electron counts in the cluster (14 for main-group Z), the electronics that come with Z ($\sim$24 elements all told), the number of countercations that must be suitably bound in the cluster array, the relative sizes of all of the components as these affect packing and structure, and a range in the number of extra outer halide atoms X^a that are bound at the six vertices of each metal octahedron. In the main family of these compounds, the X^a parameter may vary from six [viz., $(M_6X_{12}Z)X^a_6$] to zero ($M_6X_{12}Z$), the difference from six being met by the further bonding of inner (X^i) halide in other clusters in a shared mode (X^{i-a}) or, on rare occasion, by more exotic sharing means, e.g., X^{a-a-a}.

The dependence of structure and general stability on the halide used (Cl, Br, I) may also be relatively marked. As first investigated for zirconium clusters, the chlorides exhibit a large variety of compounds and structures while the iodides are much more limited in number, basically to the two charge types $Zr_6I_{14}Z$ and $Zr_6I_{12}Z$ and some alkali-metal derivatives. The rare-earth element clusters show a large variety but in the opposite sense, the cluster chlorides being rather sparse compared with numerous iodide varieties (e.g., 3, 4). In each family of metal cluster halides, the bromides were at first expected to be somehow intermediate between chlorides and iodides. But the fine subtleties of size and concomitant variations in the stabilities of alternate products have shown this to be otherwise (at least to the extent that all definitive experiments have been tried). Thus, bromides of yttrium and scandium (but not praseodymium) seem to be richest in structures containing $R_{16}Br_{20}Z_4$-type cluster oligomers (5–7), while zirconium bromides afford several apparently unique constructions. Among the latter, we have earlier reported a new tunnel structure for $A_5Zr_6Br_{15}Be$ (A = Rb, Cs) (8), a stuffed rhombohedral perovskitic network in $Cs_3Zr_6Br_{15}Z$ (Z = B, C) (9), and lastly, phases with A = K or Cs in which the first examples of extra halide is accommodated in A_4Br^{3+} tetrahedra within suitable networks (10). (Another example of the A_4X^{3+} has now been found in $K_4La_6I_{14}Os$ (11).) We report here another bromide-unique structure in $K_4Zr_6Br_{18}C$, which contains isolated $(Zr_6(C)Br^i_{12}Br^a_6)^{4-}$ cluster anions in a new arrangement. Some new $A_xZr_6Br_xZ$-type phases with x = 17, 16, 15, 14, and 12 that are isotypic with known chloride or iodide compounds are also described more briefly, particularly as they differ in stability characteristics, cation content, and so forth.

EXPERIMENTAL SECTION

The Zr metal source, the production of 100-mesh powdered Zr, the synthesis and purification of $ZrBr_4$, the

0022-4596/98 $25.00

handling of reactants and products in gloveboxes, the reaction techniques in welded Ta containers, and the characterization means have been described before (8, 9). Guinier powder X-ray diffraction was again used for precise lattice parameter determinations, phase identification, and yield estimates. The B and Be employed were stated to be 5–9's and 3–9's in purity, respectively (Aldrich), while the C was spectroscopic-grade graphite (Union Carbide), and the Mn chips (4–9's) came from Johnson-Matthey. Reagent-grade LiBr, NaBr, KBr, RbBr, CsBr were each first dried under high vacuum and then sublimed.

Syntheses

$K_4Zr_6Br_{18}Z$: The carbide phase was first recognized as dark purple needles formed during a reaction of stoichiometry $K_2Zr_6Br_{10}C$ at 820°C for 4 weeks. After the composition had been established by the structure analysis, a like reaction with stoichiometric proportions provided >90% yield of the phase. Substitution of Na for K gave an unknown product. According to the structural information obtained for the carbide (below), the Guinier powder pattern of the isostructural $K_4Zr_6Br_{18}Fe$ was also identified after the appropriate reaction, the pattern indexed, and the lattice constants refined as $a = 10.178(2)$ Å, $b = 10.358(3)$ Å, $c = 10.454(3)$ Å; $\alpha = 118.40(2)^\circ$, $\beta = 100.43(2)^\circ$, $\gamma = 103.54(2)^\circ$, $V = 885.7(3)$ Å^3.

Other studies of reduced zirconium bromide systems produced compounds that were isostructural with chlorides or iodides already reported. Only the respective synthetic conditions and any restrictions are reported in Table 1; their structure types, dimensional data, and unique features will be described later.

TABLE 1
Synthesis Conditions for Other Types of New Bromide Cluster Phases

Compound	Conditions[a] (°C, d)	Comments
$BaZr_6Br_{17}B$	900°, 40 (+$AlBr_3$)	No carbide with Ba or Ca
$Cs_4Zr_6Br_{16}Be$	750°, 141; 800°, 14	Low temp. phase relative to $Cs_{4.6}Zr_6Br_{15}Be$[b]
$Na_3Zr_6Br_{16}B$	820°, 40	Excess Zr required; e.g., from a $Na_2Zr_6Br_9B$ composition
(K,Rb)$Zr_6Br_{15}Be$	820°, 21	
$AZr_6Br_{14}Z$ (A = Li–Cs, Z = B, C, Mn)	850°, 21	
$Zr_6Br_{12}Z$, Z = Be, B	850°, 14	No carbide could be formed

[a] On-stoichiometry syntheses unless noted.
[b] Reference (8).

Single Crystal Studies

One of the acicular crystals of $K_4Zr_6Br_{18}C$ found in the products of the initial reaction (above) was used to characterize its structure. Data collection was performed with the aid of a CAD4 diffractometer and Mo$K\alpha$ radiation. A hemisphere of data to $2\theta < 55^\circ$ was collected for the indicated triclinic cell with an ω–θ scan mode. An empirical absorption correction was performed with the aid of three ψ-scan measurements. The reflection intensity statistics indicated a centric cell, and the duplicate observed reflections ($I > 3\sigma_I$) so averaged with $R_{ave} = 3.1\%$. Some important data collection and refinement parameters are given in Table 2. The model provided by direct methods in SHELXS-86 (12) contained all of the Zr, Br, and C positions, and two K sites were found in the difference Fourier map after isotropic refinement of the Zr and Br positions. Isotropic refinement of all the heavy atom parameters gave $R(F) = 8.1\%$ and $R_w = 7.9\%$, and anisotropic refinements smoothly converged at $R = 5.1\%$ and $R_w = 4.7\%$. Occupancies of the K positions refined along the way did not differ from 100% by 1σ and were fixed at unity thereafter. The refined atom positions and anisotropic atom displacement parameters are compiled in Table 3.

TABLE 2
Crystal Data for $K_4Zr_6Br_{18}C$

Space group, Z	$P\bar{1}$ (no. 2), 1
Cell parameters,[a] Å, (°)	
a	10.114(2)
b	10.283(3)
c	10.374(3)
α	118.54(2)
β	99.98(2)
γ	104.08(2)
V (Å^3)	864.5(3)
Crystal dimens. (mm)	$0.03 \times 0.05 \times 0.32$
Diffractometer, radiation	CAD4, Mo$K\alpha$
Octants measufred	$h, \pm k, \pm l$
2θ (max) (°)	55
Reflections	
Meas.	4187
Observed ($I/\sigma_I > 3.0$)	1603
Indep.	1512
Abs. coeff. (Mo$K\alpha$, cm^{-1})	228.08
Transm. coeff. range	0.59–1.00
R_{ave}, % (obs.)	3.1
No. variables	129
Sec. extinct. coeff. (10^{-6})	1.1(3)
R,[b] %	5.1
R_w,[b] %	4.7
Largest residual, e/Å^3	1.6 (1.75 Å from Br1)

[a] Guinier powder data with Si as an internal standard, 23°C.
[b] $R = \sum ||F_o| - |F_c|| / \sum |F_o|$; $R_w = [\sum w(|F_o| - |F_c|)^2 / \sum w(F_o)^2]^{1/2}$; $w = \sigma_F^{-2}$.

TABLE 3
Positional and Thermal Parameters Data for $K_4Zr_6Br_{18}C$ ($P\bar{1}$)

Atom	x	y	z	B_{eq} (Å^2)	U_{11}[a]	U_{22}	U_{33}	U_{12}	U_{13}	U_{23}
Zr1	0.3547(3)	0.2612(3)	0.9550(3)	1.8(1)	22(2)	20(2)	23(2)	5(1)	6(1)	11(2)
Zr2	0.3503(3)	0.4440(3)	0.7699(3)	1.75(9)	20(2)	22(2)	21(2)	7(1)	5(1)	10(1)
Zr3	0.3611(3)	0.6258(3)	0.1323(3)	1.6(1)	20(2)	20(2)	21(2)	10(1)	8(1)	9(1)
Br1	0.1723(3)	0.5786(4)	0.8876(4)	2.5(1)	25(2)	37(2)	32(2)	17(2)	8(2)	17(2)
Br2	0.4929(3)	0.0816(4)	0.7985(4)	2.4(1)	30(2)	19(2)	38(2)	10(2)	13(2)	11(2)
Br3	0.1752(3)	0.3690(4)	0.0989(4)	2.4(1)	28(2)	31(2)	39(2)	12(2)	18(2)	19(2)
Br4	0.5033(3)	0.2911(4)	0.2133(4)	2.5(1)	32(2)	32(2)	33(2)	5(2)	5(2)	22(2)
Br5	0.4864(3)	0.2905(4)	0.5825(3)	2.6(1)	30(2)	42(2)	20(2)	17(2)	9(2)	12(2)
Br6	0.1636(3)	0.1577(4)	0.6812(3)	2.4(1)	25(2)	26(2)	27(2)	2(2)	2(2)	11(2)
Br7	0.1754(3)	0.9696(4)	0.8988(4)	3.0(1)	38(2)	27(2)	43(2)	4(2)	14(2)	20(2)
Br8	0.1647(3)	0.3776(4)	0.4913(4)	3.1(1)	36(2)	42(2)	29(2)	11(2)	−3(2)	17(2)
Br9	0.1972(3)	0.7787(4)	0.2915(4)	3.1(1)	41(2)	40(2)	46(2)	25(2)	27(2)	21(2)
K1	0.1880(8)	0.724(1)	0.5636(9)	4.3(3)	54(5)	54(6)	54(5)	20(4)	23(4)	28(5)
K2	0.1546(9)	0.039(1)	0.2285(9)	4.7(3)	54(5)	54(6)	54(5)	20(4)	23(4)	28(5)
C	1/2	1/2	0	4(1)	83(6)	60(6)	55(5)	48(5)	32(5)	34(5)

[a] $U_{ij} \times 10^3 \cdot T = \exp[-2\pi^2(U_{11}h^2a^{*2} + U_{22}k^2b^{*2} + U_{33}l^2c^{*2} + 2U_{12}hka^*b^* + 2U_{13}hla^*c^* + 2U_{23}klb^*c^*)]$.

RESULTS AND DISCUSSION

$K_4Zr_6Br_{18}C$

As expected from the formula type, $K_4Zr_6Br_{18}C$ contains isolated $[Zr_6(C)Br^i_{12}](Br^a_6)^{4-}$ clusters that are interspersed with K^+ ions in a relatively simple extended structure. Although the cell is triclinic, it contains only one cluster per cell and the packing is fairly regular. The contents and surroundings of one cell are shown in Fig. 1, the isolated centric cluster is illustrated in Fig. 2 with the atom numbering scheme, and an extended [010] section (viewed normal to the a–c plane) appears as Fig. 3. The last illustration is actually an edge-on view of layers of clusters, and the comparable [001] section (normal to the a–b plane) looks very similar save for a 4.1° change in the angle between the axes ($\beta \rightarrow \gamma$). The cluster layers are, as seen, stacked in an irregular way along [100], but eclipsed along $\vec{a}$, of course.

The cluster itself is relatively undistorted from octahedral symmetry, and it is the modes by which the cations are bound that give this phase a unique structure, yet one which is demonstrably related to those of similar chloride compositions with larger cations. The distances and angles in Table 4 reveal how close the present centric cluster is to octahedral symmetry. The overall ranges of Zr–Zr and

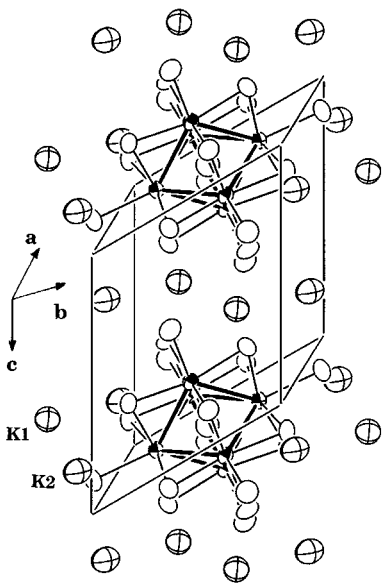

FIG. 1. The structure of $K_4Zr_6Br_{18}C$ in and around the triclinic unit cell (80% probability ellipsoids). The Zr and K atoms are shaded and crossed, respectively.

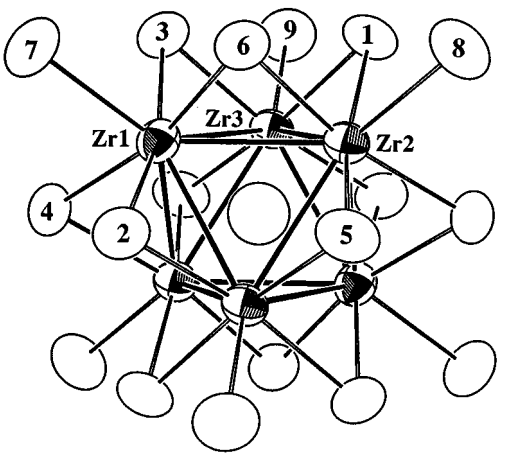

FIG. 2. The centric $[Zr_6(C)Br^i_{12}]Br^{a\,4-}_6$ cluster with the atom numbering scheme. (The C atom is unmarked.) (90%).

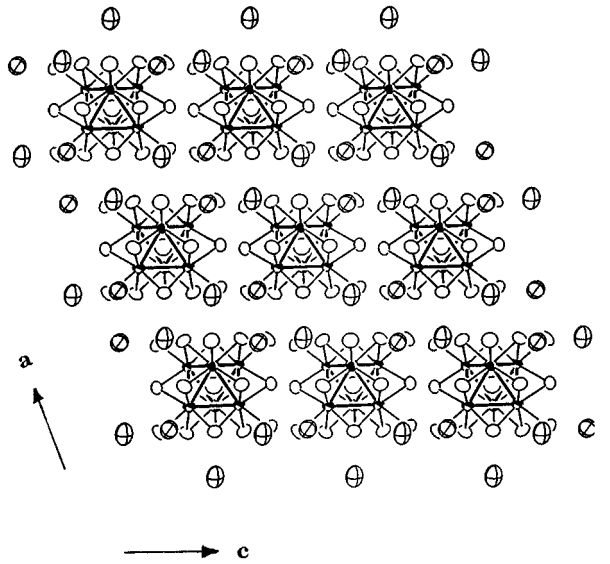

FIG. 3. [010] projection of the $K_4Zr_6Br_{18}C$ structure showing cluster layers normal to a^* with potassium atoms within their bromine surfaces (90%).

Zr–C distances are only at the 2.6 and 3.5 σ levels (0.015 Å), while the breadth of d(Zr–Bi^i) and d(Zr–Br^a) are only 7σ. Some of these variations arise because of interactions between cluster bromides and the cations that give rise to the rather unusual packing. Close inspection of Fig. 3 shows that the K1 and K2 cations (crossed ellipsoids) lie neither in the annulus between nor within the cluster layers but nearly in the same plane as the six bromine atoms at the end of each cluster (Fig. 2), while a second nonmetal layer is defined by Br2, 4, 5 plus the carbon interstitial and cuts through the cluster waists. This layering can be seen in the x coordinates of the K, Br, C components which group around 0.155–0.197 and 0.486–0.503, respectively. (In detail, the former layer of 6Br and K1 is 0.33 Å wide (center to center), and K2 lies 0.09 Å outside of this.) [100] projections of the atoms that lie about $x = 1/6$ and 1/2 do not show a regular close-packing arrangement but only wavy rows of atoms, some of the disruption in the first coming because of the smaller size of K^+ relative to Br.

These irregularities in cluster dimensions, the potassium layering, and the low symmetry cluster stacking are presumably all caused by what is necessary to accommodate potassium cations in good bonding environments. Table 4 shows that the K1 environment contains $4Br^a + 2Br^i$, the two secondary Br^i additional neighbors being 0.3 Å farther away ($\sim$3.57 Å), while K2 is four-bonded only to Br^a, the more basic (less bonded) of the bromine atom types, the $\bar{d}$ = 3.22 Å comparing with 3.31 Å from standard radii (13). (Recall that each of the Br^a is also bonded to a zirconium atom.) Figure 4 shows the unusual arrangements around both K1 (A) and K2 (B), each of which is generated by bromine from four neighboring clusters. The four Br^a about K1 are in fact close to trigonal pyramidal with the cation only 0.09 Å out of the basal plane, while the customarily longer Br^i separations fill out the other hemisphere. (The still longer, dashed interaction with Br5 is 3.86 Å.) The K2 interactions (Fig. 4B) are principally with 4Br^a in a squashed tetrahedral array. The lesser degree of distortion leaves K2 farther from Br^i in all four clusters, the four next closer K–Br^i separations at 3.72–3.99 Å being marked with dashed lines.

The singular lack of significant cation interactions with Br1^i is logically reflected in slightly shorter Zr–Br1^i distances among all of this type (Table 4). Further correlations of distance with cation contacts (or other) are not very good, perhaps because the distance range over the whole group is small relative to the errors. Among the Zr–Br^a distances,

TABLE 4
Important Bond Distances (Å) and Angles (°) in $K_4Zr_6Br_{18}C$

d(Zr–Zr)			d(K–Br)	
Zr1–Zr2	2 ×	3.258(4)	K1–Br9	3.144(8)
	2 ×	3.269(4)	–Br8	3.203(8)
–Zr3	2 ×	3.270(4)	–Br7	3.226(8)
	2 ×	3.273(4)	–Br8	3.325(8)[b]
Zr2–Zr3	2 ×	3.269(4)	–Br2	3.506(8)
	2 ×	3.270(4)	–Br4	3.632(8)
$\bar{d}$		3.270	$\bar{d}$	3.339
			K2–Br9	3.151(8)
d(Zr–C)			–Br8	3.196(8)
Zr1–C		2.306(3)	–Br7	3.200(8)
Zr2–C		2.309(3)	–Br7	3.332(8)[b]
Zr3–C		2.321(3)	$\bar{d}$	3.220
$\bar{d}$		2.312		
			d(Br–Br)[a]	
d(Zr–Br^i)			Br1–Br8	3.587(5)
Zr1–Br2		2.679(4)	Br1–Br9	3.606(6)
–Br3		2.663(4)	Br3–Br7	3.611(5)
–Br4		2.669(4)	Br6–Br7	3.612(4)
–Br6		2.673(4)	Br3–Br9	3.625(5)
Zr2–Br1		2.647(4)	Br4–Br7	3.630(5)
–Br4		2.671(4)		
–Br5		2.687(4)		
–Br6		2.680(4)	Zr2–Zr1–Zr2	90.1(2)
Zr3–Br1		2.650(4)	Zr2–Zr1–Zr3	59.98(8)
–Br2		2.675(4)	Zr3–Zr1–Zr3	90.4(1)
–Br3		2.667(4)	Zr1–Zr2–Zr3	60.03(9)
–Br5		2.686(4)	Zr3–Zr2–Zr3	90.3(1)
$\bar{d}$		2.670	Zr1–Zr3–Zr1	89.6(1)
d(Zr–Br^a)			Br2–Zr1–Br3	165.2(1)
Zr1–Br7		2.817(4)	Br4–Zr1–Br6	165.0(1)
Zr2–Br8		2.820(5)	Br1–Zr2–Br5	165.4(1)
Zr3–Br9		2.772(5)	Br4–Zr2–Br6	165.4(1)
$\bar{d}$		2.803	Br1–Zr3–Br5	165.4(1)
			Br2–Zr3–Br3	165.9(1)

[a] d(Br–Br) < 3.64 Å.
[b] More parallel to [001], Fig. 4.

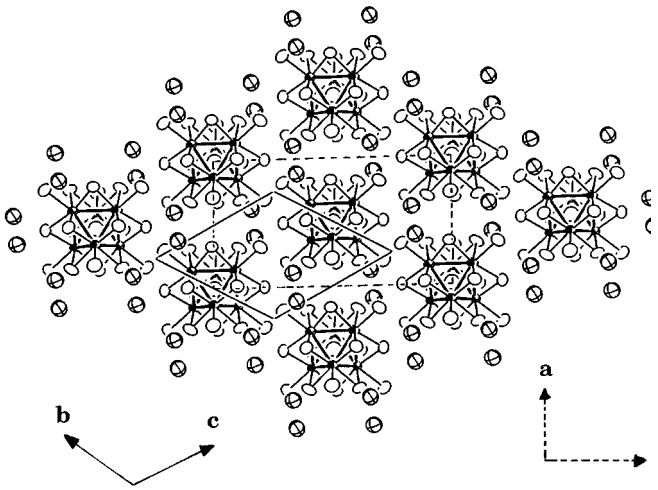

FIG. 4. [100] projection of a cluster layer in $K_4Zr_6Br_{18}C$. The face of the triclinic cell is marked in solid lines, and that of the pseudo-C-centered cell, in dashed lines (see text).

TABLE 5
Lattice Dimensions for Three Structurally Related $A_nZr_6Cl_{18}Z$ Phases

	$Rb_5Zr_6Cl_{18}B$[a]	$Rb_4Zr_6Cl_{18}C$[b]	$K_4Zr_6Br_{18}C$
Space group ($Z = 2$)	*Pman*	*C*2/*m*	$C\bar{1}$[c]
a (Å)	10.941(4)	10.460(4)	10.114(2)
b	17.769(4)	17.239(4)	17.757(5)
c	9.078(5)	9.721(4)	10.556(3)
α (°)	90.00	90.00	90.58(2)
β	90.00	115.05(3)	114.04(3)
γ	90.00	90.00	92.27(3)
V(Å^3)	1760(1)	1588.0(9)	1729(2)
Layer repeat, Å	9.08	8.81	9.64

[a]Ref. 15.
[b]Ref. 14.
[c]The pseudo-C-centered monoclinic cell transformed from the true triclinic cell by (1 0 0; 0 1 −1; 0 1 1).

that to Br9 is distinctly shorter as it has only two rather than three cation neighbors.

Related Structures

Although $K_4Zr_6Br_{18}C$ exhibits a new structure, it is possible to find distinct relationships with the structures of monoclinic $Rb_4Zr_6Cl_{18}C$ (14) and orthorhombic $Rb_5Zr_6Cl_{18}B$ (15). Their common feature is the distinct layering of the clusters. A [100] projection normal to the cluster layer in the present compound is shown in Fig. 4. Outlined thereon are the faces of the proper triclinic cell (solid lines) and a quasi-C-centered monoclinic cell (dashed) into which the former can be approximately transformed. The result is analogous to the precise C-centered arrangement of the cluster layers in the related monoclinic $Rb_4Zr_6Cl_{18}C$ (as well as in the nominally isotypic $K_4Nb_6X_{18}$, $X = Cl$, Br (16,17) (*C*2/*m*). The comparative lattice dimensions of all three compounds, the last based on the pseudo-*C*1 version of the present structure, are detailed in Table 5. The cluster layers in C-centered $Rb_4Zr_6Cl_{18}C$ are stacked along a *c* axis that is inclined 115° to the indicated (dashed) $\vec{a}$, while in triclinic $K_4Zr_6Br_{18}C$ these are translated along an *a* axis that is inclined 104° and 100° to the indicated $\vec{b}$ and $\vec{c}$, respectively.

The analogous Rb atoms in the former ruby-colored chloride are crystallographically all of one type and again lie in the outer halide layers on the clusters. Moreover, the Rb atoms are again surrounded by $4Cl^a$ plus $2Cl^i$ with an overall geometry and distance spectrum that is remarkably similar to K1 here. These are compared in Fig. 5A, $K_4Zr_6Br_{18}C$, and Fig. 5C, $Rb_4Zr_6Cl_{18}C$. There is no analog of K2 in the latter. The smaller cations and larger clusters are presumably responsible for the lower symmetry found in the potassium bromide phase. It should be noted that $K_4Nb_6Cl_{18}$ does not occur in the present $K_4Zr_6Br_{18}C$ structure, presumably because of its smaller cluster; rather, it crystallizes in parallel with $Rb_4Zr_6Cl_{18}C$. The average six-bonded Rb–Cl and K1–Br distances (Fig. 5) are essentially the same, in agreement with crystal radii expectations, so matrix effects (nonbonded Br••Br repulsions) do not seem important. However, further details of "cause and effect" are difficult to discern.

To some degree, these structural relationships carry on to $Rb_5Zr_6Cl_{18}B$ as well. Now comparable cluster layers are stacked eclipsed (•• AA •••) in an orthorhombic cell, and there are three types of four-fold Rb^+ sites, the third being half occupied and disordered. The molar volume increase from $Rb_4Zr_6Cl_{18}C$ to $Rb_5Zr_6Cl_{18}B$, 52 cm^3, well exceeds the expected cation increment for Rb^+, 20 cm^3 (18), a sign that this phase is less well packed. (The increase in cluster volume because of the change in Z is only $\sim$1 cm^3.) Disorder in the relatively poor site for Rb3 is further support for this observation. Site Rb1 is now a larger, nine-coordinate position (with only $3Cl^a$) that lies between the clusters within the layers. Furthermore, though Rb2 has $4Cl^a$ and $2Cl^i$ neighbors, as do K1 here and Rb in $Rb_4Zr_6Cl_{18}B$, it lies about midway between the cluster layers and with a $\bar{d}$(Rb2–Cl) value that is 0.04 Å and 0.07 Å larger than $\bar{d}$(K1–Br) and d(Rb–Cl) in the other two, respectively, another sign of less adequate bonding. The individual cluster layers in $Rb_5Zr_6Cl_{18}B$ are again approximately close packed. The relationship of $Rb_5Zr_6Cl_{18}B$ to the other two considered here is clearly more distant, and the reason for the eclipsed stacking of the cluster layers, difficult to fathom.

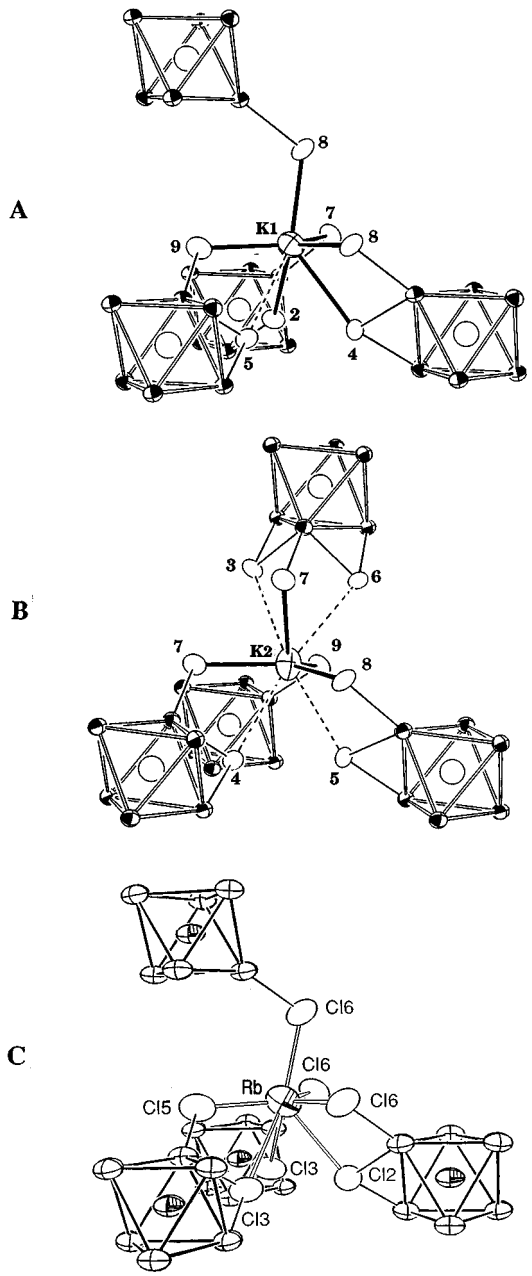

FIG. 5. The nearest cluster and bonded bromine environments around (A) K1 and (B) K2 in $K_4Zr_6Br_{18}C$ (c^* vertical, 70%). (C) The cation environment in $Rb_4Zr_6Cl_{18}C$, closely similar to that for K1 in (A) (reprinted with permission from Ref. 14).

Other Zirconium Bromides with Known Structures

The studies that led to several examples each of the above and four other new structure types (8–10) for quaternary zirconium bromides also turned up a good number of isotypes of structures previously reported for zirconium chloride or iodide cluster compounds. Table 6 summarizes lattice dimensions and structure types for the 17 new bromide compounds of known structure. Six of these have been refined from single crystal data, and the results are available on request from J.D.C. The following discussion covers mainly examples on this list that exhibit unusual or different stability relationships, stoichiometries, or matrix effects.

All known $A_xZr_6X_{16}Z$-type phases contain puckered layers with a $(Zr_6X_{12}Z)X^{a-a}_{4/2}X^a_2$ connectivity in which the four vertices about the waist of each cluster are halogen-bridged to others, while the trans-vertices contain only X^a. These layers appear to be puckered largely in order to afford good cation sites. The previously characterized $Cs_3Zr_6Cl_{16}C$ (20) is a more reduced 15-electron version of $Cs_4Zr_6Br_{16}Be$ (14e). Isotypic chlorides with Z = B, Be were also obtained at the time, but the cation content was not established, and it is reasonable that one (Be) or both achieved a general composition closer to that established here, $Cs_4Zr_6Br_{16}Be$. The extra cesium atom present in the bromide formulation is accommodated by full occupation of the two sites that were fractionally filled $Cs_3Zr_6Cl_{16}C$, a feature that was in effect forced by the provision of only the electron-richer carbon as Z. Attempts to produce the analogous bromide boride gave instead two other phases, $Cs_3Zr_6Br_{15}B$ (9) or $(Cs_4Br)Zr_6Br_{16}Be$ (6), depending on the Cs content.

Because of a change in interstitial, just the converse in compositional variation is found in orthorhombic $Na_3Zr_6Br_{16}B$ relative to the nominally isotypic $Na_4Zr_6Cl_{16}Be$ characterized before (20). Here a comparable half occupancy of the less basic Na2 site occurs while the least favorable Na3 position surrounded only by Br^i is left empty. As before, excess Zr is necessary to gain this structure, while the stoichiometric reaction gives an unknown phase. Attempts to prepare the $Na_4Zr_6Br_{16}Be$ analog gave instead the novel $(Na_4Br)_2Zr_6Br_{18}Be$ (10).

The monoclinic structure of $Rb_3Zr_6Br_{15}Be$ is basically the same as $K_3Zr_6Cl_{15}Be$, which in turn is a distorted version of $K_2Zr_6Cl_{15}B$ required to accommodate the extra cation forced by the use of Be for Z. The bromide appears to exhibit some clear matrix effects relative to the chloride beryllide; short intracluster Br3–Br7 and Br8–Br8 distances of 3.496(2) and 3.547(3) Å are presumably most of the reason for the expansion of the cluster core, 0.043 Å (21σ) in d(Zr–Be) and the corresponding 0.060 Å increase in $\bar{d}$(Zr–Zr) to 3.360 Å.

The $Zr_6X_{14}Z$ ($\simeq Nb_6Cl_{14}$ (25)), $AZr_6X_{14}Z$, and $Zr_6X_{12}Z$ compositions and structures are relatively common and pervasive in all of the zirconium (and some hafnium (26)) halide systems. The preparation of a series of $AZr_6Br_{14}Z$ phases, A = Li–Cs, Z = B, C, Mn is as expected from the chlorides already known, yet contrasting with the iodides where the A range is limited (23, 27, 28). The $LiZr_6Br_{14}B$ member affords another, rare example of a structural change in which a small A cation is placed in an alternate site. The vast majority of quaternary $AZr_6X_{14}Z$ examples

TABLE 6
New Zirconium Bromide Cluster Phases That Are Nominally Isotypic with Other Zirconium Halide Compounds

Compound	Space group (No)	Lattice Constants (Å, deg.)[a]				Parent Str.	Ref.
		a	*b*	*c*	*β*		
$BaZr_6Br_{17}B$[b]	*I*4/*m* (87)	12.0406(5)		10.3180(5)		$BaZr_6Cl_{17}C$	19
$Cs_4Zr_6Br_{16}Be$[b]	$P2_1/c$ (14)	11.493(2)	12.465(2)	14.591(2)	122.08(1)	$Cs_3Zr_6Cl_{16}C$	20
$Na_3Zr_6Br_{16}B$[b]	*Pccn* (56)	13.869(1)	14.720(1)	14.5814(7)		$Na_4Zr_6Cl_{16}Be$	20
$K_3Zr_6Br_{15}Be$	*C*2/*c* (15)	17.143(2)	11.9115(7)	14.716(2)	92.424(9)	$K_3Zr_6Cl_{15}Be$	21
$Rb_3Zr_6Br_{15}Be$[b]	*C*2/*c* (15)	17.232(1)	12.0407(6)	14.7067(8)	92.834(6)	$K_3Zr_6Cl_{15}Be$	21
$LiZr_6Br_{14}B$	*Cmca* (64)	14.954(1)	13.2904(9)	12.0531(9)		$LiZr_6Cl_{14}Mn$	22
$NaZr_6Br_{14}B$	*Cmca* (64)	14.789(1)	13.311(1)	12.045(1)		$CsZr_6I_{14}C$	23
$KZr_6Br_{14}B$	*Cmca* (64)	14.7906(9)	13.2961(8)	12.0576(8)		$CsZr_6I_{14}C$	23
$RbZr_6Br_{14}B$	*Cmca* (64)	14.807(2)	13.297(1)	12.117(1)		$CsZr_6I_{14}C$	23
$CsZr_6Br_{14}B$	*Cmca* (64)	14.827(2)	13.306(2)	12.184(2)		$CsZr_6I_{14}C$	23
$NaZr_{16}Br_{14}C$	*Cmca* (64)	14.6876(9)	13.2266(8)	11.9864(8)		$CsZr_6I_{14}C$	23
$RbZr_6Br_{14}C$	*Cmca* (64)	14.719(1)	13.287(1)	12.043(1)		$CsZr_6I_{14}C$	23
$LiZr_6Br_{14}Mn$[c]	*Cmca* (64)	15.193(4)	13.473(5)	12.271(3)		$CsZr_6I_{14}C$	23
$NaZr_6Br_{14}Mn$[c]	*Cmca* (64)	15.390(7)	13.675(5)	12.228(5)		$CsZr_6I_{14}C$	23
$CsZr_6Br_{14}Mn$[b]	*Cmca* (64)	15.062(1)	13.483(2)	12.387(1)		$CsZr_6I_{14}C$	23
$Zr_6Br_{12}Be$[b]	$R\bar{3}$ (148)	13.7094(6)		9.3242(5)		$Zr_6I_{12}C$	23
$Zr_6Br_{12}B$[b]	$R\bar{3}$ (148)	13.6348(6)		9.3057(6)		$Zr_6I_{12}C$	2
							2

[a]Data from Guinier powder patterns with Si as internal standard; $\lambda = 1.540\,562$ Å, 22°C.
[b]Single crystal data refined.
[c]Ref. (24).

bind the cation in a large 12-coordinate site, but $LiZr_6Cl_{14}Mn$ was first demonstrated to have the cation bound instead in a six-coordinate pseudo-octahedral position. This presumably occurred in order to avoid its "rattling" in the usual site, even though use of the new Li^+ site requires some *expansion* of the lattice, its cell volume ($Z = 4$) of 2198 Å^3 being greater than those of the $Zr_6Cl_{14}Mn$ ternary (2187) Å^3, $KZr_6Cl_{14}Mn$ (2173 Å^3), and the rubidium analogue (2182 Å^3). Apparently $NaZr_6Cl_{14}Mn$ is also a member of the minority (2216 Å^3). The same behavior has been deduced in the $AZr_6Cl_{14}B$ phases, A = Li–Cs, Tl, but only for lithium (29). The present compounds (Table 6) do not show this deviation for $AZr_6Br_{14}Mn$ (V(Li) = 2512(1) Å^3, V(Na) = 2574(2) Å^3), but they certainly do for $LiZr_6Br_{14}B$ (2395.5(3) Å^3) where the cell is again distinctly larger than for Na, K (2371.2(1) Å^3) and Rb (2385.6 Å^3). This presumably arises because of the smaller size of B vs Mn as this affects cavity sizes in the presence of the larger bromide. The cell volume increment from B to Mn with fixed Z is 108–112 Å^3 in the chlorides and bromides.

The $Zr_6Br_{12}Z$ examples (Z = B, Be) are the first for which dimensional data are available for a bromide. These are nicely intermediate in this structure type, and some matrix effects are readily evident. The 15-e $Zr_6Cl_{12}B$ could not be obtained (30), but $Zr_6Br_{12}B$ can. Likewise, we could not gain the 16-e $Zr_6Br_{12}C$, but $Zr_6I_{12}C$ is well known. Increased distortion of the cluster unit through both increasing halide size and smaller Z (matrix effects) consistently makes the a_{1u} LUMO level (in the 14-e O_h description) less antibonding and more susceptible to occupation when forced (in part) by the choice of the size variables (15). Distortion in this case specifically means further withdrawal of metal vertices from the plane defined by the four neighboring X^i bridges, which lessens π^* components in a_{1u}.

Conclusion

The effects that atom sizes, stoichiometry, and electronic details have on stability and structure among the many $A_xZr_6X_{12+x}Z$ compounds continue to be a source of both amazement and further understanding of subtle details and their interrelationships. The question of phase stability is one of the major challenges in solid state chemistry, and this multifaceted cluster collection does much to teach us what is, and can be, important. Additional novelties can be uncovered when mixed halogens are used to differentiate requirements and possibilities among nonequivalent positions and functions (30, 31). Notwithstanding these extensive investigations, five additional structures among the bromide results remain as unknown powder patterns because no analogy with phases in other systems could be found and adequate monocrystals were not obtained.

ACKNOWLEDGMENTS

This research was supported by the National Science Foundation, Solid State Chemistry, via Grants DMR-9207361 and -9510278 and was carried out in the facilities of the Ames Laboratory, U.S. Department of Energy.

REFERENCES

1. J. D. Corbett, *in* "Modern Perspectives in Inorganic Crystal Chemistry" (E. Parthé, Ed.) (NATO ASI Series C), p. 27. Kluwer Academic, Dordrecht, the Netherlands, 1992.
2. J. D. Corbett, *J. Alloys Compd.* **229,** 10 (1995).
3. M. Lulei, J. D. Martin, L. M. Hoistad, and J. D. Corbett, *J. Am. Chem. Soc.* **119,** 513 (1997).
4. Y. Park, J. D. Martin, and J. D. Corbett, *J. Solid State Chem.* **129,** 277 (1997).
5. S. J. Steinwand and J. D. Corbett, *Inorg. Chem.* **35,** 7056 (1996).
6. S. J. Steinwand, J. D. Corbett, and J. D. Martin, *Inorg. Chem.* **36,** 6413 (1997).
7. R. Llusar and J. D. Corbett, *Inorg. Chem.* **33,** 849 (1994).
8. R.-Y. Qi and J. D. Corbett, *Inorg. Chem.* **34,** 1646 (1995).
9. R.-Y. Qi and J. D. Corbett, *Inorg. Chem.* **34,** 1657 (1995).
10. R.-Y. Qi and J. D. Corbett, *Inorg. Chem.* **36,** 6039 (1997).
11. S. Uma and J. D. Corbett, unpublished research, 1998.
12. G. M. Sheldrick, SHELXS-86, Programs for Structure Determination. Universität Göttingen, Germany, 1986.
13. R. P. Shannon, *Acta Crystallogr. Sect. A* **32,** 751 (1976).
14. J. Zhang, R. P. Ziebarth, and J. D. Corbett, *Inorg. Chem.* **31,** 614 (1992).
15. R. P. Ziebarth and J. D. Corbett, *J. Am. Chem. Soc.* **111,** 3272 (1989).
16. A. Simon, H. G. von Schnering, and H. Schäfer, *Z. Anorg. Allg. Chem.* **361,** 235 (1968).
17. F. Ueno and A. Simon, *Acta Crystallogr. Sect. C* **41,** 308 (1985).
18. W. Biltz, *in* "Raumchemie der festen Stoffe," p. 120. L. Voss, Leipzig, Germany, 1934.
19. J. Zhang and J. D. Corbett, *J. Less-Common Met.* **156,** 49 (1989).
20. R. P. Ziebarth and J. D. Corbett, *Inorg. Chem.* **28,** 626 (1989).
21. R. P. Ziebarth and J. D. Corbett, *J. Am. Chem. Soc.* **110,** 1132 (1988).
22. J. Zhang and J. D. Corbett, *J. Solid State Chem.* **109,** 265 (1994).
23. J. D. Smith and J. D. Corbett, *J. Am. Chem. Soc.* **107,** 5704 (1985).
24. R. Llusar and J. D. Corbett, unpublished results.
25. A. Simon, H. G. Schnering, H. Wöhrle, and H. Schäfer, *Z. Anorg. Allg. Chem.* **339,** 155 (1965).
26. R.-Y. Qi and J. D. Corbett, *Inorg. Chem.* **33,** 5727 (1994).
27. J. D. Smith and J. D. Corbett, *J. Am. Chem. Soc.* **108,** 1927 (1986).
28. T. Hughbanks, G. Rosenthal, and J. D. Corbett, *J. Am. Chem. Soc.* **110,** 1511 (1988).
29. R. P. Ziebarth and J. D. Corbett, *J. Solid State Chem.* **80,** 56 (1989).
30. M. Köckerling, R.-Y. Qi, and J. D. Corbett, *Inorg. Chem.* **35,** 1437 (1996).
31. M. Köckerling, *Inorg. Chem.* **37,** 380 (1998).